Acadlore Transactions on AI and Machine Learning
https://www.acadlore.com/journals/ATAIML

Microwave Detection System for Wheat Moisture Content Based on Metasurface Lens Antennas

Suping Yu, Weiwei Mao*

College of Computer and Information Engineering, Luoyang Institute of Science and Technology, 471023 Luoyang, China

* Correspondence: Weiwei Mao (mw116@lit.edu.cn)

Received: 08-22-2024 **Revised:** 10-02-2024 **Accepted:** 10-08-2024

Citation: S. P. Yu and W. W. Mao, "Microwave detection system for wheat moisture content based on metasurface lens antennas," *Acadlore Trans. Mach. Learn.*, vol. 3, no. 4, pp. 193–201, 2024. https://doi.org/10.56578/ataiml030401.

Abstract: Maintaining wheat moisture content within a safe range is of critical importance for ensuring the quality and safety of wheat. High-precision, rapid detection of wheat moisture content is a key factor in enabling effective control processes. A microwave detection system based on metasurface lens antennas was proposed in this study, which facilitates accurate, non-invasive, and contactless measurement of wheat moisture content. The system measures the attenuation characteristics of wheat with varying moisture content from 23.5 GHz to 24.5 GHz in the frequency range. A linear regression equation (coefficient of determination R^2=0.9946) was established by using the measured actual moisture content obtained through the standard drying method, and was used as the prediction model for wheat moisture. Totally, 72 wheat samples were selected for moisture content prediction, yielding a root mean square error (RMSE) of 0.193%, mean absolute error (MAE) of 0.16%, and maximum relative error (MRE) of 5.25%. The results indicate that the proposed microwave detection system, based on metasurface lens antennas, provides an effective method for detecting wheat moisture content.

Keywords: Wheat; Moisture content; Metasurface lens antenna; Microwave detection

1 Introduction

The moisture content of wheat has a direct impact on its stability during transportation, storage, and processing. Excessive moisture content can increase the germination rate of wheat and make it more susceptible to insect infestation and mould growth, while low moisture content can increase breakage rates and negatively affect both the sowing and consumption quality of the wheat [1]. Therefore, accurate detection of wheat moisture content and maintaining it within a safe range are essential for ensuring wheat quality and safety. Detection methods for wheat moisture content are generally classified into direct and indirect methods. The former includes the oven-drying and chemical drying methods, which offer high accuracy but are time-consuming and complex, making them unsuitable for real-time online detection. Indirect methods primarily include capacitance methods [2], high-frequency impedance methods [3], near-infrared methods [4, 5], and nuclear magnetic resonance methods [6]. While each of these methods has its own advantages, they also come with certain limitations.

Microwave detection systems, which rely on changes in the amplitude, phase, and frequency of electromagnetic waves caused by the interaction between microwaves and wheat [7], offer a non-contact, non-destructive, and rapid means of measuring wheat moisture content. Extensive research on the use of microwaves for detecting grain moisture content has been conducted by scholars both domestically and internationally. For instance, Wu and Zhu [8] employed ground-penetrating radar to study the attenuation characteristics of electromagnetic waves in relation to wheat moisture content within grain silos, thereby enabling non-contact detection of moisture content during storage. Another study by Guo et al. [9] utilised horn-lens antennas to convert spherical waves into plane waves, establishing a free-space transmission method to detect wheat moisture content. Zhang et al. [10] designed a rapid, non-contact moisture detection device for peanuts, combining a vector network analyser with a horn-lens antenna, thus achieving non-destructive detection of peanut moisture content. Furthermore, Zhang et al. [11] and Sun et al. [12] utilised the sweep frequency method to obtain transmission loss and phase data at different frequencies, and combined these with a deep neural network algorithm to measure moisture content in sweet corn and rice. Although these microwave detection systems provide rapid, non-contact measurement of grain moisture content, the large size and high manufacturing

cost of the equipment present significant limitations for practical application. Metasurface lens antennas, which are characterised by high-gain radiation, high efficiency, flexible radiation performance, miniaturisation, and ease of manufacture, are widely used in radar communication and microwave detection systems [13–15]. Based on the advantages of metasurface lens antennas, a compact and integrated microwave detection system for wheat moisture content was designed in this study. This system allows for high-precision, non-destructive, and non-contact detection of wheat moisture content.

2 System Components and Methodology

2.1 Detection System Design

The proposed microwave detection system primarily investigates the attenuation of microwaves as they propagate through wheat samples, and a linear regression prediction model for wheat moisture content was established based on the attenuation characteristics of samples with varying moisture content. According to Figure 1, the measurement setup consists of two 24 GHz metasurface lens antennas housed within a measurement enclosure. These antennas are used for the transmitting and receiving antennas, respectively, and they are connected to a vector network analyser via coaxial cables. The metasurface lens antennas comprise a feed antenna and a metasurface lens, which convert the spherical waves emitted by the feed antenna into plane waves, thereby reducing measurement errors caused by diffraction effects at the sample edges. A foam container filled with wheat was placed between the two antennas, ensuring that the distances from the container's outer cross-section to each antenna are identical. The container has internal dimensions of 100 mm×100 mm×60 mm. The measurement enclosure was constructed from acrylic plates, and absorbing material was applied to the interior surface to minimise reflection interference between the enclosure and the antennas. The vector network analyser measures the transmission coefficient S21, while a computer receives and processes the data. Based on the attenuation characteristics of wheat with varying moisture content, the data were linearly fitted to the actual moisture content obtained using the standard drying method [16–19], thus establishing the linear regression prediction model for wheat moisture content. The attenuation characteristics were determined by the difference in attenuation, ΔA, of microwave propagation with and without the wheat sample. The attenuation difference ΔA was derived using Eqs. (1)-(3) [20, 21].

$$S_{21} = |S_{21}|\, e^{\mathrm{j}\varphi} \tag{1}$$

$$A = -20 \lg |S_{21}| \tag{2}$$

$$\Delta A = A_w - A_{air} \tag{3}$$

where, A represents the attenuation (dB), φ denotes the phase angle, A_w is the attenuation with the wheat sample present, A_{air} is the attenuation without the wheat sample, and ΔA is the attenuation difference.

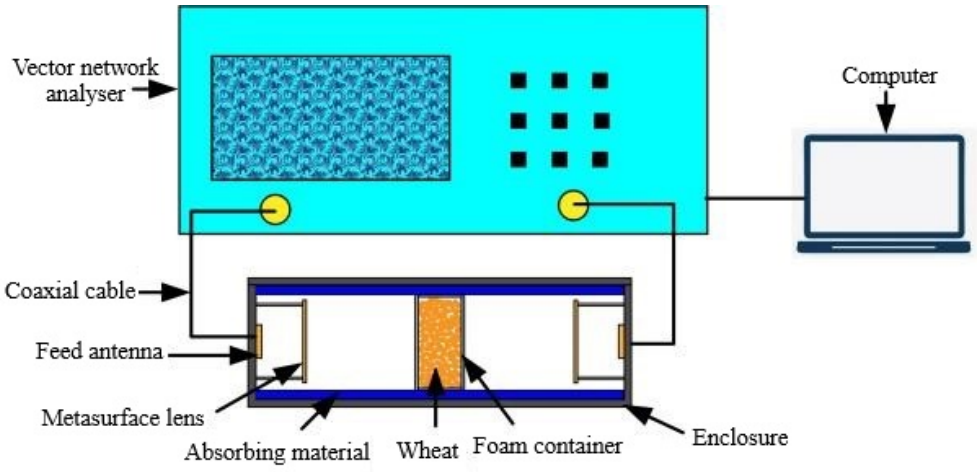

Figure 1. Schematic of the microwave detection system

2.2 Metasurface Lens Antenna Design

The designed metasurface lens antenna in this study has two main components, i.e., the feed antenna and the metasurface lens. The feed antenna is a rectangular microstrip patch antenna positioned at the focal point of the lens.

The metasurface lens is composed of hexagonal transmission units arranged in a stepped configuration. As shown in Figure 2, each transmission unit was constructed from four identical layers of metallic microstrip patches and three dielectric substrates. Each metallic microstrip patch layer consists of a circular patch and a hexagonal ring. The metal layer is 0.035 mm in thickness, and the dielectric substrate is made of Arlon AD255C material, with 2.65 and 0.0014 being the relative permittivity and loss tangent. Each dielectric substrate layer is 0.762 mm in thickness. The side length a of the hexagonal unit is 3 mm, and the line of the hexagonal ring is 0.1 mm in width. The radius r of the internal circular metallic patch can be adjusted to modify the transmission unit's transmission amplitude and phase.

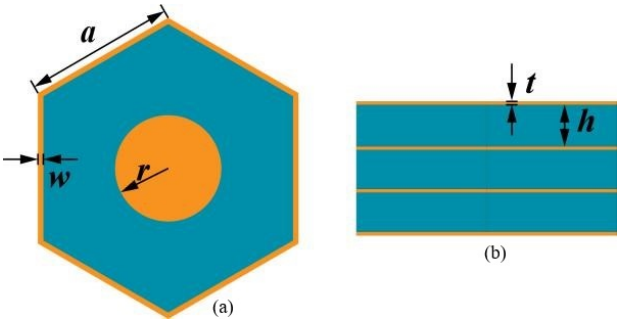

Figure 2. Structure of the transmission unit: (a) Front view; (b) Side view

The transmission unit was modelled using Ansys HFSS software, with master-slave boundary conditions applied to ensure the perpendicular incidence of plane waves. A comprehensive parametric study was conducted to analyse the transmission unit's transmission amplitude and phase at 24 GHz in frequency. Figure 3 shows the optimised parameter results. It can be observed that by varying the radius r of the circular patch to 2.1 mm from 0.3 mm, the transmission phase can be adjusted from -180° to 180°, covering a total phase range of 360°. Additionally, the transmission amplitude of the unit remains above 0.83. Notably, within the phase ranges of [-180°, -139°] and [-82°, 180°], the transmission amplitude exceeds 0.9.

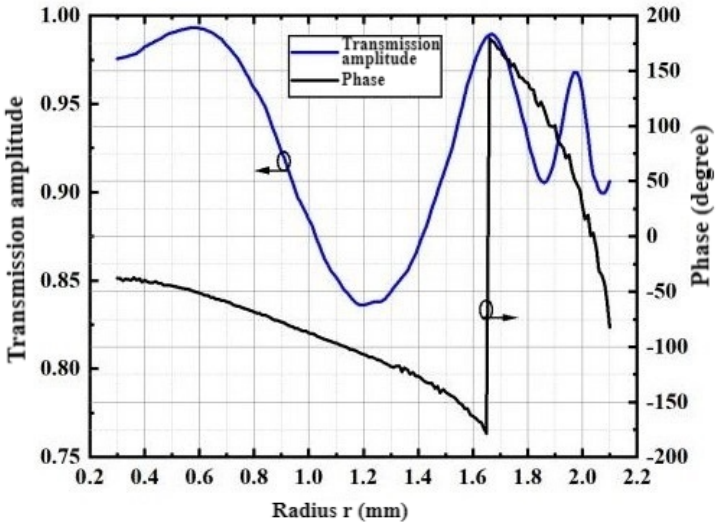

Figure 3. Transmission characteristic curves of the unit

As shown in Figure 4, the physical structure of the metasurface lens antenna includes the metasurface transmission array, feed antenna, and nylon support columns. The metasurface transmission array consists of 241 hexagonal transmission units. The arrangement of the transmission units within the lens array is determined primarily by the phase delay from the feed antenna to each unit. The transmission phase compensation required at different positions is determined by Eq. (4).

$$\varphi(x,y) = (2\pi/\lambda_0)\left(\sqrt{x^2+y^2+f^2} - f^2\right) + \varphi_0 \tag{4}$$

where, φ_0 represents the phase of the central unit. The central unit's centre is taken as the origin, with x and y representing the horizontal and vertical coordinates of each unit's centre relative to the origin. The central frequency

is 24 GHz, and the wavelength λ_0 in free space is 12.49 mm. The focal length, denoted as f, is 30 mm. When the radius r of the circular metallic patch is 1.65 mm, the transmission unit's transmission amplitude is 0.98, and the transmission phase φ_0 is -180°. This transmission unit was selected as the central unit to ensure a high transmission amplitude at the centre of the lens array.

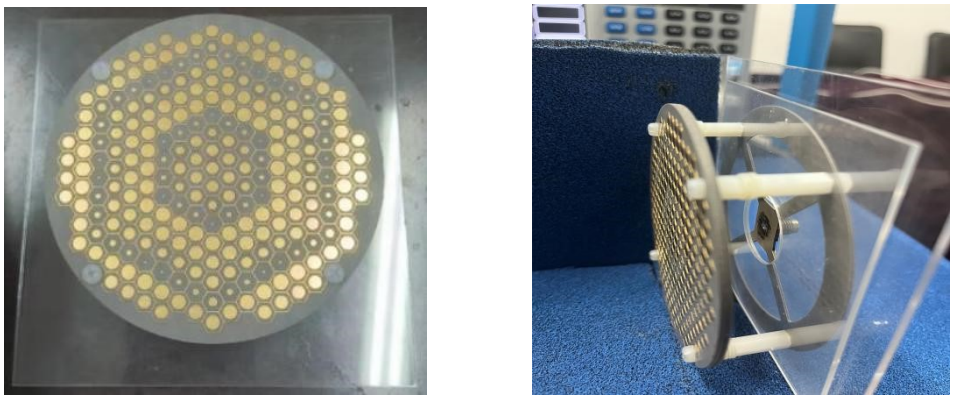

(a) (b)

Figure 4. Metasurface lens antenna structure: (a) Metasurface lens array; (b) Complete metasurface lens antenna

The measured reflection coefficients of the feed antenna and the metasurface lens antenna are shown in Figure 5. It can be observed that the rectangular microstrip patch antenna exhibits a reflection coefficient (S_{11}<-10 dB) from 23 GHz to 25 GHz in the frequency range. Similarly, the metasurface lens antenna demonstrates a reflection coefficient (S_{11}<-10 dB) from 23.25 GHz to 25 GHz within the frequency range.

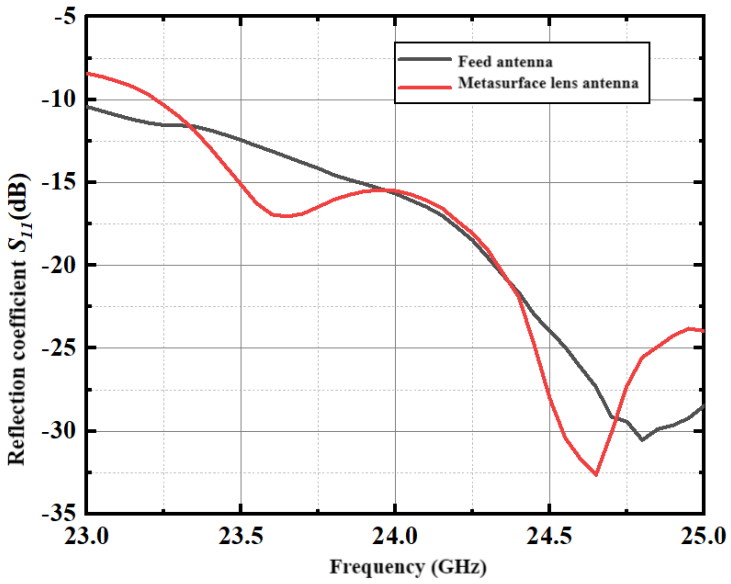

Figure 5. Comparison of the reflection coefficients of the feed antenna and the metasurface lens antenna

Figure 6 shows the simulated electric field distribution of the metasurface lens antenna in the xoz plane. It can be observed that the metasurface lens antenna is capable of transforming the spherical waves emitted by the feed antenna into plane waves. Figure 7 compares the simulated radiation patterns of the feed and metasurface lens antennas at 24 GHz. The metasurface lens antenna achieves 21.35 dBi peak gain, representing an improvement of 15.5 dBi over the peak gain of the feed antenna alone. Additionally, compared to the feed antenna, the metasurface lens antenna's half-power beamwidth is reduced by 71° in the xoz plane and by 76° in the yoz plane.

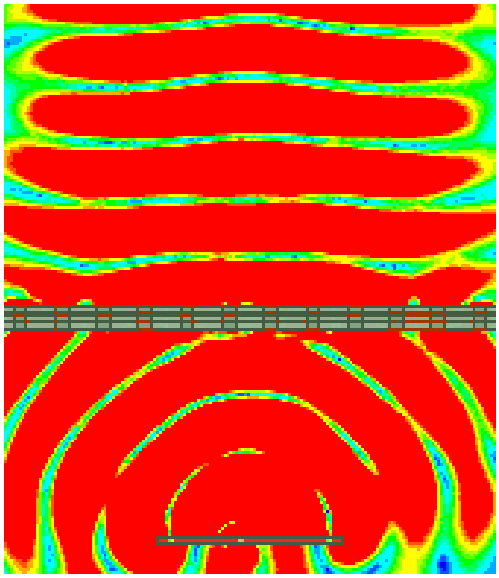

Figure 6. Electric field diagram of the metasurface lens antenna

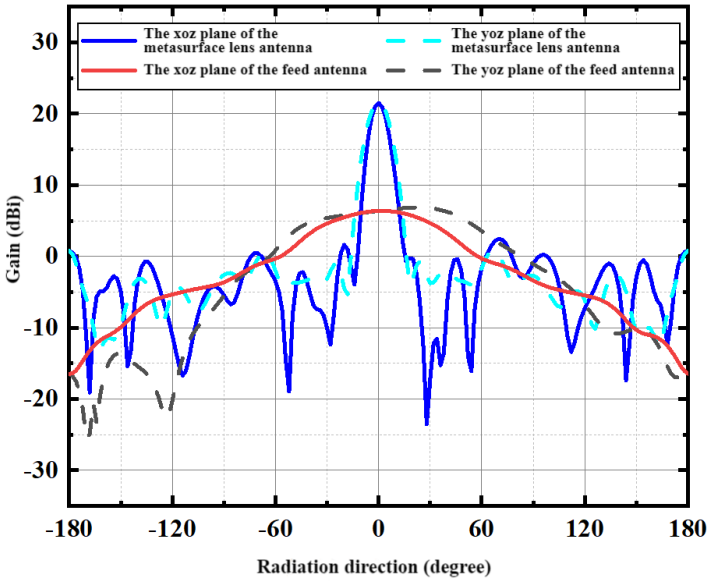

Figure 7. Comparison of the radiation patterns of the feed and metasurface lens antennas

3 Experiment

3.1 Experimental Materials

The wheat samples (Zhengmai 379) used in this experiment were harvested in June 2021 in Zhengzhou, Henan Province. The moisture content of the wheat, determined using the standard drying method, was initially 14.4%. The wheat samples were dried in batches in an oven at 30°C for varying durations, resulting in 80 wheat samples prepared at eight different moisture content levels. The prepared samples were sealed, classified, and stored in a refrigerator at 5°C. To minimise the influence of temperature on the experimental results, the wheat samples were kept at room temperature (25°C) for more than 48 hours before measurements.

3.2 Experimental Procedure

As shown in Figure 8, the microwave detection system for measuring wheat moisture content has an overall size of 300 mm × 120 mm × 120 mm. The microwave frequency range of the vector network analyser was between 23.5 GHz and 24.5 GHz. Eight wheat samples, which had different moisture contents, were selected as the test set, and their microwave attenuation values were measured. The wheat samples were placed into the container via free fall, ensuring the container was filled and positioned equidistantly between the transmitting and receiving antennas.

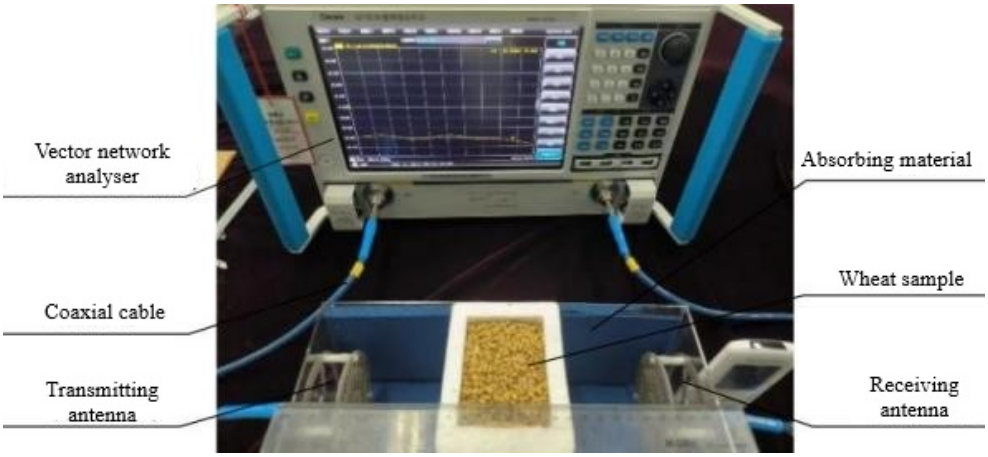

Figure 8. Internal structure of the microwave detection system for wheat moisture content

4 Results and Analysis

Figure 9 shows the relationships between the attenuation variation characteristics and the frequency for wheat samples with different moisture contents. When the frequency ranges between 23.5 GHz and 24.5 GHz, the attenuation variation characteristics exhibit a linear relationship with the wheat moisture content. The corresponding attenuation variation also increases when the wheat moisture content becomes larger.

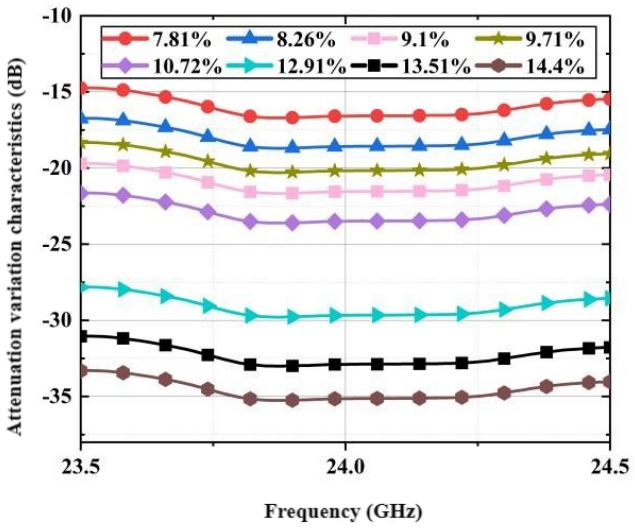

Figure 9. Attenuation variation characteristics of wheat with different moisture contents from 23.5 GHz to 24.5 GHz in the frequency range

Based on the linear relationship observed between attenuation variation characteristics and the actual wheat moisture content in the test set, a linear regression equation can be fitted.

$$\Delta A = bM + c \tag{5}$$

where, M represents the wheat moisture content, ΔA is the microwave attenuation difference, c is the intercept, and b is the regression coefficient. The coefficient of determination $\left(\mathrm{R}^2\right)$ determines the linear regression equation's degree of fit. When the $\left(\mathrm{R}^2\right)$ value is closer to 1, the regression equation fits the data better. As shown in Figure 10, the actual wheat moisture content was fitted with the attenuation difference, yielding a coefficient of determination of 0.9946, a regression coefficient b of -2.592, and an intercept c of 2.427. The fitting results indicate that the linear regression equation ΔA=-2.592M+2.427, which describes the relationships between the attenuation variation characteristics and the actual moisture content of wheat samples from 23.5 GHz to 24.5 GHz in the frequency range, can be used as a predictive model for wheat moisture content.

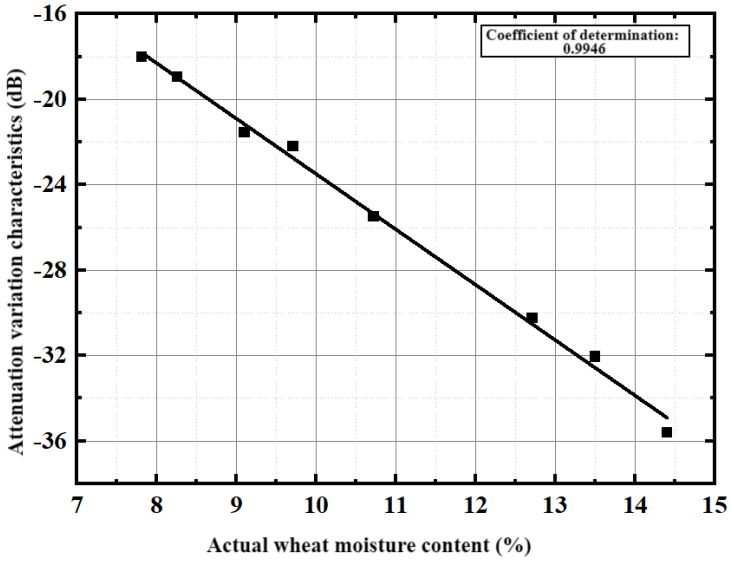

Figure 10. Fitting results of actual wheat moisture content and attenuation variation characteristics

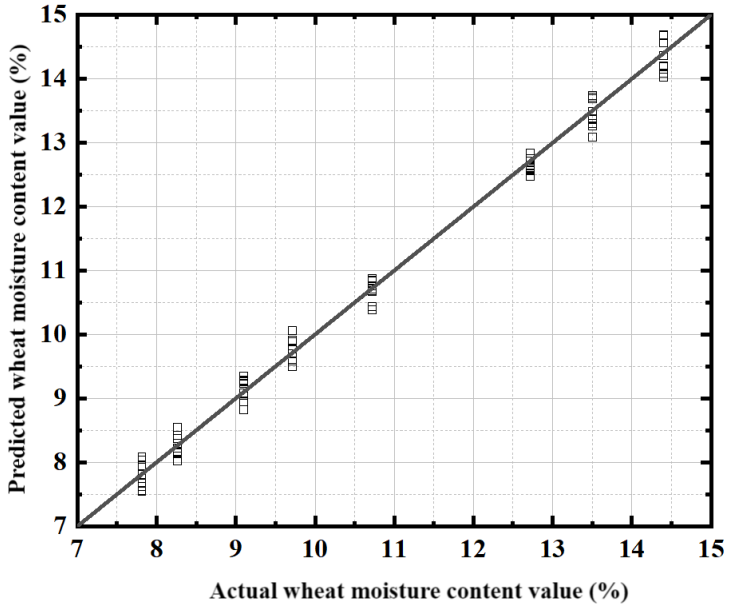

Figure 11. Comparison of actual and predicted wheat moisture content values

Based on the linear regression equation established in this experiment, the attenuation variation characteristics measured from the wheat samples can be substituted into the equation to predict the moisture content. For the moisture content ranging between 7.81% and 14.4%, the remaining 72 wheat samples were selected as the prediction set. Figure 11 shows the prediction results. The RMSE of the predicted wheat moisture content is 0.193%, the MAE is 0.16, and the MRE is 5.25%. These measurement results indicate that the proposed microwave detection system can measure wheat moisture content with high accuracy.

5 Conclusions

A microwave detection system for wheat moisture content based on a metasurface lens antenna was proposed in this study, enabling high-precision, non-destructive, and non-contact measurement of wheat moisture content. The main findings and conclusions are as follows:

(a) A metasurface lens antenna with a centre frequency of 24 GHz was designed. A microstrip patch antenna was used as the feed antenna, and the metasurface lens successfully converted the spherical waves emitted by the feed antenna into plane waves, improving the peak gain by 15.5 dB compared with the feed antenna alone. The use of the metasurface lens antenna instead of a traditional horn-lens antenna better meets the requirements for miniaturisation

and integration in microwave detection systems for wheat moisture content.

(b) Through the microwave detection system developed in this study, the attenuation variation characteristics of wheat samples were measured and a linear regression equation was established to correlate these characteristics with the actual moisture content of the wheat. This equation can serve as a prediction model for wheat moisture content, with the prediction results yielding 0.193% RMSE, 0.16 MAE, and 5.25% MRE. These results indicate that the wheat moisture content detection system developed in this study is an effective method for measuring wheat moisture content and holds potential for advancing the miniaturisation and integration of microwave detection systems for future applications.

Funding

The research was funded by the Henan Province Science and Technology Key Project (Grant No.: 242102210127) and the Key Research Project of Higher Education Institutions in Henan Province (Grant No.: 24B510008).

Data Availability

The data used to support the research findings are available from the corresponding author upon request.

Conflicts of Interest

The authors declare no conflict of interest.

References

[1] M. Homayoonfal and N. Malekjani, "Drying of cereal grains and beans," *Drying Technol. Food Process.*, pp. 459–489, 2023. https://doi.org/10.1016/B978-0-12-819895-7.00009-2

[2] I. M. Naguib and S. A. Ragheb, "Achieving sustainability in smart cities & its impact on citizen," *Int. J. Sustain. Dev. Plan.*, vol. 17, no. 8, pp. 2621–2630, 2022. https://doi.org/10.18280/ijsdp.170831

[3] G. W. Chang and H. J. Lu, "Integrating gray data preprocessor and deep belief network for day-ahead PV power output forecast," *IEEE Trans. Sustain. Energy*, vol. 11, no. 1, pp. 185–194, 2018. https://doi.org/10.1109/TSTE.2018.2888548

[4] Y. Wang and Y. Lu, "Evaluating the potential health and economic effects of nitrogen fertilizer application in grain production systems of China," *J. Clean. Prod.*, vol. 264, p. 121635, 2020. https://doi.org/10.1016/j.jclepro.2020.121635

[5] P. Agrafioti, E. Kaloudis, S. Bantas, V. Sotiroudas, and C. G. Athanassiou, "Modeling the distribution of phosphine and insect mortality in cylindrical grain silos with computational fluid dynamics: Validation with field trials," *Comput. Electron. Agric.*, vol. 173, p. 105383, 2020. https://doi.org/10.1016/j.compag.2020.105383

[6] H. Ghafori, "Computational fluid dynamics (CFD) analysis of pipeline in the food pellets cooling system," *J. Stored Prod. Res.*, vol. 87, p. 101581, 2020. https://doi.org/10.1016/j.jspr.2020.101581

[7] Z. K. Zhao and C. Z. Wu, "Wheat quantity monitoring methods based on inventory measurement and SVR prediction model," *Appl. Sci.*, vol. 13, no. 23, p. 12745, 2023. https://doi.org/10.3390/app132312745

[8] H. Wu and X. M. Zhu, "Short-term electric load forecasting model based on PSO-BP," in *2023 4th International Conference on Big Data, Artificial Intelligence and Internet of Things Engineering*, Hangzhou, China, 2023, pp. 224–228. https://doi.org/10.1109/ICBAIE59714.2023.10281261

[9] X. G. Guo, Q. N. Zhao, D. Zheng, Y. Ning, and Y. Gao, "A short-term load forecasting model of multi-scale CNN-LSTM hybrid neural network considering the real-time electricity price," *Energy Rep.*, vol. 6, pp. 1046–1053, 2020. https://doi.org/10.1016/j.egyr.2020.11.078

[10] Q. Q. Zhang, W. Li, H. K. Li, X. H. Chen, M. Jiang, and M. S. Dong, "Low-field nuclear magnetic resonance for online determination of water content during sausage fermentation," *J. Food Eng.*, vol. 212, pp. 291–297, 2017. https://doi.org/10.1016/j.jfoodeng.2017.05.021

[11] X. X. Zhang, H. Zhang, Z. Q. Wang, X. Chen, and Y. Chen, "Research on the temperature field of grain piles in underground grain silos lined with plastic," *J. Food Process Eng.*, vol. 45, no. 3, p. e13971, 2022. https://doi.org/10.1111/jfpe.13971

[12] S. G. Sun, Z. T. Wen, T. H. Du, J. Q. Wang, Y. Tang, and H. Gao, "Remaining life prediction of conventional low-voltage circuit breaker contact system based on effective vibration signal segment detection and MCCAE-LSTM," *IEEE Sens. J.*, vol. 21, no. 19, pp. 21 862–21 871, 2021. https://doi.org/10.1109/JSEN.2021.3104290

[13] Y. Du, J. L. Wang, and J. G. Lu, "Optimization of magnetically coupled resonant wireless power transfer based on improved whale optimization algorithm," *J. Ind Intell.*, vol. 1, no. 1, pp. 63–74, 2023. https://doi.org/10.56578/jii010105

[14] B. Lenaerts and M. Demont, "The global burden of chronic and hidden hunger revisited: New panel data evidence spanning 1990–2017," *Glob. Food Secur.*, vol. 28, p. 100480, 2021. https://doi.org/10.1016/j.gfs.2020.100480

[15] S. Trabelsi, A. M. Paz, and S. O. Nelson, "Microwave dielectric method for the rapid, non-destructive determination of bulk density and moisture content of peanut hull pellets," *Biosyst. Eng.*, vol. 115, no. 3, pp. 332–338, 2013. https://doi.org/10.1016/j.biosystemseng.2013.04.003

[16] J. Y. Zhang, Y. Bao, D. D. Du, J. Wang, and Z. B. Wei, "OM2S2: On-line moisture-sensing system using multi-frequency microwave signals optimized by a two-stage frequency selection framework," *IEEE Trans. Ind. Electron.*, vol. 68, no. 11, pp. 11 501–11 510, 2021. https://doi.org/10.1109/TIE.2020.3032927

[17] J. Y. Zhang, C. Y. Wu, W. Q. Shao, F. Q. Yao, J. Wang, and Z. B. Wei, "Thickness-independent measurement of grain moisture content by attenuation and corrected phase shift of microwave signals at multiple optimized frequencies," *IEEE Trans. Ind. Electron.*, vol. 69, no. 11, pp. 11 785–11 795, 2022. https://doi.org/10.1109/TIE.2021.3116582

[18] H. F. Wang, Z. B. Wang, Z. H. Wu, and Y. R. Zhang, "Beam-scanning lens antenna based on elliptical paraboloid phase distribution metasurfaces," *IEEE Antennas Wirel. Propag. Lett.*, vol. 18, no. 8, pp. 1562–1566, 2019. https://doi.org/10.1109/LAWP.2019.2922695

[19] L. B. Safdar, K. Dugina, A. Saeidan, G. V. Yoshicawa, N. Caporaso, B. Gapare, M. J. Umer, R. A. Bhosale, I. R. Searle, M. J. Foulkes, S. A. Boden, and I. D. Fisk., "Reviving grain quality in wheat through non-destructive phenotyping techniques like hyperspectral imaging," *Food Energy Secur.*, vol. 12, no. 5, p. e498, 2023. https://doi.org/10.1002/fes3.498

[20] F. Cui, G. Q. Dong, B. P. Chen, P. L. Yong, and S. P. Peng, "Application of ground penetrating radar technology in moisture content detection of stored grain," *J. Agric. Eng.*, vol. 54, no. 1, p. 1472, 2023. https://doi.org/10.4081/jae.2022.1472

[21] D. Yang, Y. X. Zhou, Y. Jie, Q. Li, and T. Y. Shi, "Non-destructive detection of defective maize kernels using hyperspectral imaging and convolutional neural network with attention module," *Spectrochim. Acta Part A*, vol. 313, p. 124166, 2024. https://doi.org/10.1016/j.saa.2024.124166